The size and shape of three water-soluble, non-ionic polysaccharides produced by lactic acid bacteria: A comparative study

Marianne Øksnes Dalheim[a], *Nina Bjørk Arnfinnsdottir*[b], *Göran Widmalm*[c], *Bjørn E. Christensen*[d*]

[a] NOBIPOL, Department of Biotechnology, Norwegian University of Science and Technology (NTNU), N-7491 Trondheim, Norway. Email: marianne.dalheim@ntnu.no

[b] Department of Physics, Norwegian University of Science and Technology (NTNU), N-7491 Trondheim, Norway. Email: nina.arnfinnsdottir@ntnu.no

[c]Department of Organic Chemistry, Arrhenius Laboratory, Stockholm University, S-106 91 Stockholm, Sweden. Email: gw@organ.su.se

[d] NOBIPOL, Department of Biotechnology, Norwegian University of Science and Technology (NTNU), N-7491 Trondheim, Norway. Email: bjorn.e.christensen@ntnu.no, telephone: + 47 73 59 33 27, fax: +47 73 59 12 83.

[*] Corresponding Author

ABSTRACT.

Three water-soluble, non-ionic extracellular polysaccharides (EPS) obtained from lactic acid bacteria (*S. thermophilus* THS, *L. helveticus* K16 and *S. thermophilus* ST1) were subjected to a comparative study by means of multidetector size-exclusion chromatography, providing distributions and averages of molar masses, radii of gyration and intrinsic viscosities. All polysaccharides displayed random coil character. Further analysis of the data reveals differences in chain stiffness and extension that could be well correlated to structural features. The calculated persistence lengths ranged from 5-10 nm and fall within the range typical for many single-stranded bacterial or plant polysaccharides. The ST1 polysaccharide had the highest molar mass but the lowest persistence length, which is attributed to the presence of the flexible (1→6)-linkage in the main chain.

KEYWORDS:

Lactic acid bacteria - EPS - SEC-MALLS - Intrinsic viscosity - persistence length

1 INTRODUCTION

Lactic acid bacteria (LAB) are used as probiotics, i.e., live microorganisms that may confer a health benefit to the host, and in production of fermented foods (Divya, Varsha, Nampoothiri, Ismail & Pandey, 2012; Patrick, 2012; Popova et al., 2012; Quigley, 2010). These gram-positive bacteria are generally regarded as safe (GRAS) and an important application is as dairy starters in production of yogurt and cheese (Patel & Prajapati, 2013). In yogurt production a number of positive effects result as a consequence of using these types of bacteria, e.g. mild flavouring, improved texture, ropiness and sensory characteristics (Purwandari, Shah & Vasiljevic, 2007). In

Mozzarella cheese-production increased moisture content and improved melting properties were regarded as positive outcomes from using a LAB strain (Broadbent, McMahon, Welker, Oberg & Moineau, 2003). It is the *in situ* production of beneficial components during fermentation that makes these probiotic LAB particularly interesting.

Microbial exopolysaccharides can be found in the cellular external environment either as capsules associated with the bacterial cell or loosely attached as slime, which may be released into the surrounding environment of the bacteria (Cescutti, 2009; Nwodo, Green & Okoh, 2012). The former type of polymeric material is referred to as a capsular polysaccharide (CPS) (Widmalm, 2013) and the latter material is in contrast often simply denoted as an exopolysaccharide (EPS) (Ruas-Madiedo, 2014). These biopolymers play a pivotal role for the bacteria in the ecological niches they populate. In particular as a physical barrier acting as a protective shield, being part of cell-cell recognition processes and colonization through biofilm formation (Ruas-Madiedo, 2014).

Two groups of exopolysaccharides can be identified in LAB strains, namely homopolysaccharides consisting of a single type of sugar residue and heteropolysaccharides having different sugar residues within the polymer (De Vuyst & Degeest, 1999; Fontana, Li, Yang & Widmalm, 2015; Nwodo, Green & Okoh, 2012). The bioactivity of the EPS is due to their action as antagonists to toxins from other bacteria; they act as a physical hindrance to the toxin targeting eukaryotic cells thereby avoiding the interaction either by blocking the toxin *per se* or by acting as a toxin-scavenger (Ruas-Madiedo, 2014; Ruas-Madiedo, Medrano, Salazar, de los Reyes-Gavilan, Perez & Abraham, 2010).

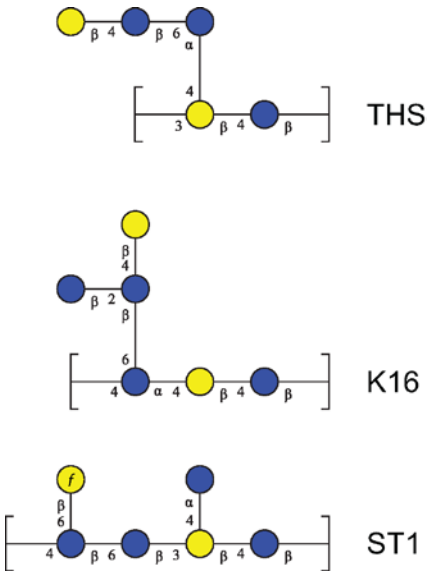

Figure 1. Schematic representation in CFG-format of the repeating units from the EPS produced by *S. thermophilus* THS, *L. helveticus* K16 and *S. thermophilus* ST1. Note the presence of lactose as a structural element in all of the backbones of the polysaccharides as well as in the THS and K16 side-chains.

Lactobacillus helveticus and *Streptococcus thermophilus* are both of the genera belonging to LAB. *S. thermophilus* THS, *L. helveticus* K16 and *S. thermophilus* ST1 produce heteropolysaccharides having glucose and galactose as constituents of the branched pentasaccharide repeating units (RUs) for the THS strain and hexasaccharide RUs for the K16 and ST1 strains (Figure 1) (Nordmark, Yang, Huttunen & Widmalm, 2005; Säwén, Huttunen, Zhang, Yang & Widmalm, 2010; Yang, Staaf, Huttunen & Widmalm, 2000). The EPS preparations used for structural determination employing in particular NMR spectroscopy gave highly viscous solutions. We herein extend the characterization of these EPS by analysing them by size exclusion chromatography with multi angle laser light scattering and viscometry (SEC-MALLS-VISC), providing information about chain extension and stiffness. It further allows a comparative analysis

between the three polysaccharides in solution (under identical conditions and with the same methodology). To our knowledge few, if any, comparisons of this type have been published for bacterial EPS.

The three polysaccharides are neutral but water-soluble. The absence of charged groups should render them largely insensitive to variations in pH and ionic strength. The physical properties are therefore expected to depend only on the geometry of the sugar residues and the glycosidic linkages, and the chain length distributions. To gain further insight into the structure-function relationships we find it useful to compare these EPS to structurally related water-soluble polysaccharides which have been thoroughly described in the literature.

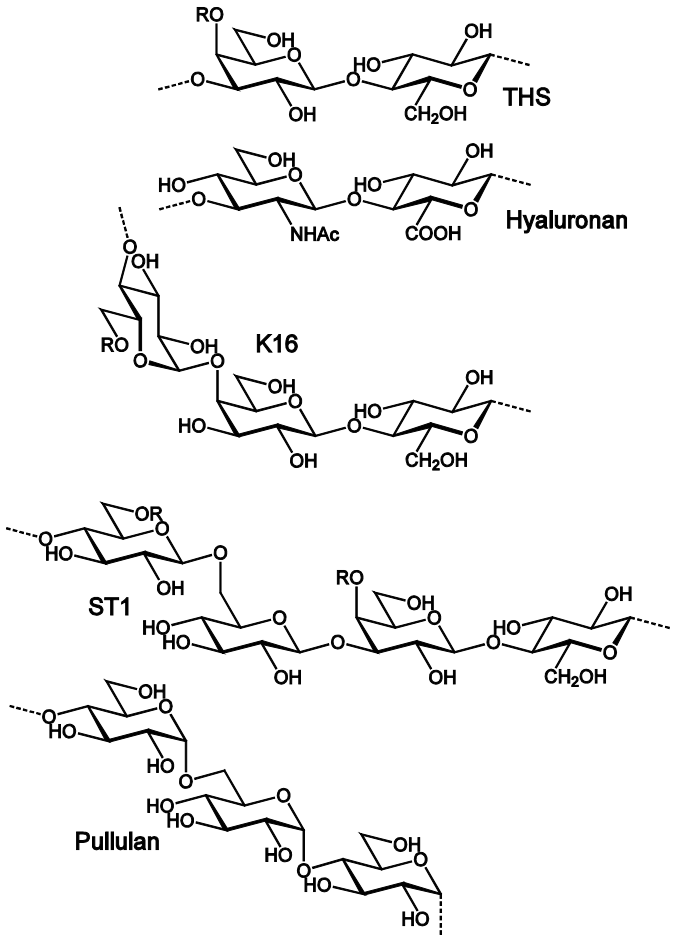

Figure 2. Chemical structures of THS, hyaluronan, K16, ST1 and pullulan polysaccharides. R denotes different side-chains.

The backbone of THS has structural similarities with hyaluronan (HA) by having a repeating disaccharide structure with alternating β-(1→3)- and β-(1→4)-linkages (Cowman & Matsuoka, 2005) (Figure 2). The differences lie in the substitution patterns: HA has a carboxylic group (intrinsic pK_a = 2.9 (Cleland, Wang & Detweiler, 1982)) due to the D-Glc*p*A residue and an N-acetyl group at position 2 of the D-Glc*p*NAc residue, whereas THS has in addition to an axial hydroxyl on C4 of the second unit a bulky trisaccharide attached to it. HA behaves in aqueous

solution as a single semi-flexible random coil with an intrinsic persistence length (at infinite ionic strength) of about 7 nm (Mendichi, Soltes & Schieroni, 2003).

The ST1 EPS has a more complex structure, where the backbone consists of a tetrasaccharide repeating unit, in addition to single side-chains on two of the residues. We did not find analogues to this particular structure, but since it contains an α-(1→6)-linkage, which is known to be particularly flexible compared to (1→3)- and (1→4)-linkages (Pendrill, Säwén & Widmalm, 2013), we found it useful to compare it to pullulan (Liu, Brant, Kitamura, Kajiwara & Mimura, 1999), which consists of maltotriose repeating units joined by α-(1→6)-linkages (Fig 2).

K16 has a backbone without (1→6)-linkages, but the diaxial α-(1→4)-linkage is expected to provide chain flexibility over the corresponding diequatorial equivalent, such as cellulose or a β-mannan backbone, for example. K16 has further a branched trisaccharide side-chain, and bears a slight structural relationship to xanthan.

In the present study we simultaneously analyse under identical experimental conditions the dilute solution properties of thee EPS from lactic acid bacteria, using multi-detector SEC analysis as previously conducted for alginates (Vold, Kristiansen & Christensen, 2006), chitosans (Christensen, Vold & Vårum, 2008), barley mixed linkage glucans (Christensen et al., 2001), and hyaluronan (Kristiansen, Dalheim & Christensen, 2013). Direct comparison to other polysaccharides with related chemical features, particularly the geometries of the backbones, was further performed.

2 MATERIALS AND METHODS

The EPS samples from *S. thermophilus* THS, *L. helveticus* K16 and *S. thermophilus* ST1 were available from the previous structural studies (Nordmark, Yang, Huttunen & Widmalm, 2005; Säwén, Huttunen, Zhang, Yang & Widmalm, 2010; Yang, Staaf, Huttunen & Widmalm, 2000). Alginate (UP-MVG) and hyaluronan were obtained from FMC Biopolymers (Oslo, Norway). Pullulan was obtained from Hayashibara (Japan).

SEC-MALLS analyses were carried out essentially as described earlier (Kristiansen, Dalheim & Christensen, 2013; Ulset, Mori, Dalheim, Hara & Christensen, 2014; Vold, Kristiansen & Christensen, 2006). In brief, the measurements were carried out at ambient temperature on an HPLC system consisting of a solvent reservoir, an online degasser, a HPLA isocratic pump, an autoinjector, a pre-column, and serially connected columns (TSK G-6000PWXL, 5000 PWXL, and 4000 PWXL). The 4000 PWXL column was omitted in some cases. The eluent was 0.05 M Na_2SO_4 containing 0.01 M NaEDTA, pH 6.0. The column outlet was connected to a Dawn DSP multi-angle laser light scattering photometer (Wyatt, U.S.A.; $\lambda 0 = 0.633$ nm) followed by an Optilab DSP differential refractometer (P-10 cell), and a ViscoStar viscosity detector. The flow rate was 0.5 mL min^{-1}. The injection volume was 100−250 μL and the sample concentration was adjusted to obtain the best possible light scattering signal without influencing the RI profile (overloading). Samples were filtered (pore size 0.22 or 0.45 μm) prior to injection. Data from the light scattering and the differential refractometer were collected and processed using Astra software (Wyatt, U.S.A.), using a refractive index increment $(dn/dc)_\mu$ of 0.150 mL g^{-1} and a first order Zimm angular fit. The general reproducibility (repeated injections of a standard sample) resulted in standard deviations of 3.5% for M_w and 6.2% for M_n (n = 4)

3 RESULTS

The multi-detector SEC data (concentration, molar mass, r.m.s. radius and intrinsic viscosity profiles) for the THS, ST1 and K16 EPS are presented in Figure 3 and the resulting summary of weight- and number average molar mass, weight average radius, and intrinsic viscosity of the three samples is presented in Table 1.

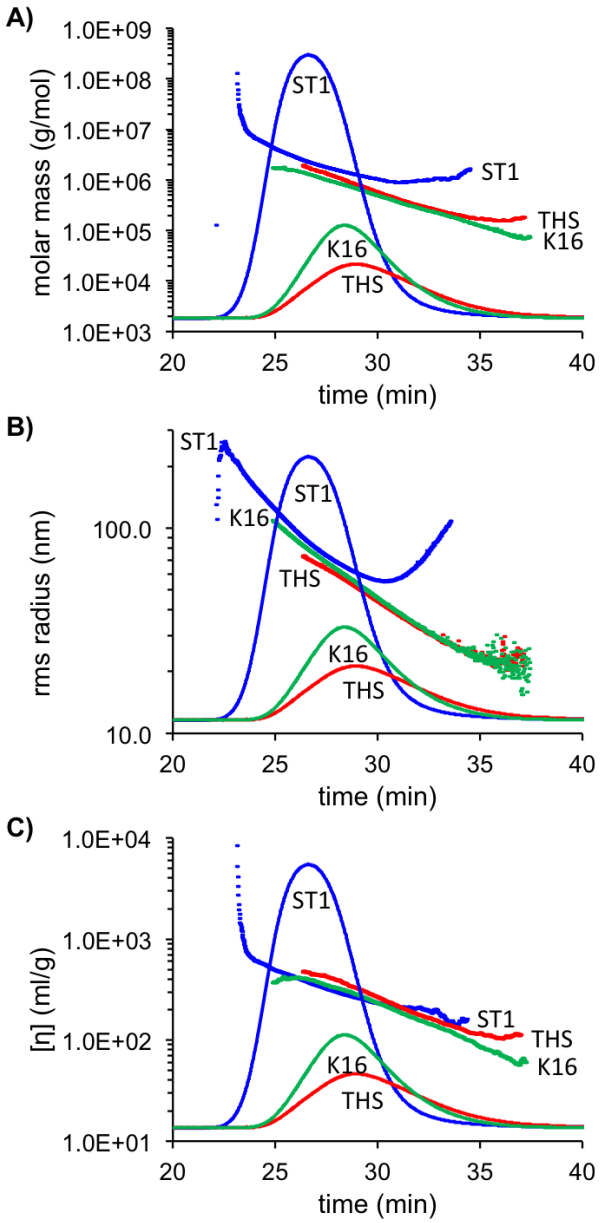

Figure 3. SEC-MALLS-VISC data: Concentration profiles, slice molecular weights (A), slice r.m.s. radii (B) and slice intrinsic viscosities (C) for THS (red), K16 (green) and ST1 (blue).

The separation according to molecular size is generally observed, although the quality of the data was not as good as normally observed for pure polysaccharides (standards, data not shown). Whereas intrinsic viscosity data in all cases showed the normal linear decrease (on a semi-logarithmic scale) with increasing elution volume, the molar mass and in particular the radius of ST1 tended to level off or even increase at the low molar mass tail. This is normally attributed to the presence of aggregates or nanoparticles, which may be caused by impurities, or by partial polysaccharide aggregation. Heat treatments did in the present case not remove these impurities. The data were therefore reprocessed by fitting the data (molar mass and R_G) to an exponential equation extrapolating downwards from the regions with normal decreasing values (Ulset, Mori, Dalheim, Hara & Christensen, 2014). As expected (Ioan, Aberle & Burchard, 2000), the effect was largest on M_n, particularly for ST1.

Table 1. Weight and number average molar mass, weight average radius of gyration (r.m.s. radius) and intrinsic viscosity (weight average) of the polysaccharides THS, K16 and ST1 as obtained by SEC-MALLS. Values in parenthesis were obtained by performing a semi-logarithmic fitting of slice data based on the linear parts of Figure 2.

	M_w (kDa)	M_n (kDa)	R_w (nm)	[η] (ml/g)
THS	490 (460)	310 (240)	40 (39)	220
K16	560 (540)	330 (310)	49 (49)	220
ST1	2200 (1940)	1700 (1060)	84 (81)	340

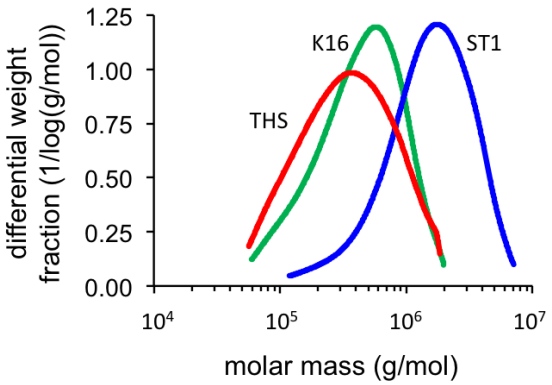

Figure 4. Molar mass distributions of THS (red), K16 (green) and ST1 (blue).

The calculated molar mass distributions are shown in Figure 4. In all three cases we observe broad distributions covering about two orders of magnitude in molar mass, and with a tendency towards tailing at low molar masses. The relative shift in distributions follows, as expected, the differences in M_w (Table 1), with ST1 be shifted to the highest molar masses, containing chains up to about 10^7 Da. The shape of the distributions are quite similar those of wide a range of polysaccharides (bacterial, algal) analysed in our laboratory, and tend to be adequately described in terms of the Kuhn distribution corresponding to partial random degradation of an infinitely long chain or random polymerization starting from monomers (Tanford, 1961). In terms of biosynthesis these distributions may correspond to specific balance between the rate of chain elongation and the rate of chain export from the cells into the extracellular surroundings.

Analysis of light scattering (Rayleigh scattering) data at each elution slice provides the radius of gyration (R_G = r.m.s. radius) without any assumptions of the shape or size of the polysaccharides, and is only limited by the wavelength of the laser, providing reasonable data down toward 20 nm below which the angular dependence on the scattered light becomes undetectable.

The classical way to compare R_G data is to plot R_G as a function of molar mass (on a double-logarithmic scale), which form basis for several types of comparisons and analyses. Data for THS, K16 and ST1 are shown in Figure 5, together with data obtained under identical experimental conditions for the reference standards alginate, hyaluronan and pullulan.

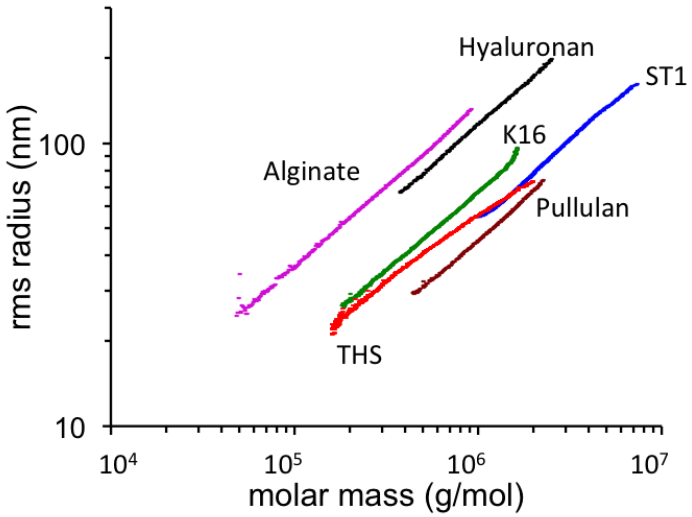

Figure 5. Molar mass dependency of R_G (slice values) for THS (red), K16 (green), ST1 (blue), alginate (magenta), HA (black) and pullulan (brown). Data at the peak ends providing pronounced deviations or noise were removed prior to analysis.

All polysaccharides except THS, but including alginate, HA and pullulan, produce perfectly straight lines with slopes in the range 0.57-0.58, in agreement with a random coil model in a thermodynamically good solvent (theoretical value 0.6).

Data for THS show a pronounced curvature, but the line is positioned between the curves for ST1 and K16, suggesting the shape and extension of the chains are rather similar. All three are

positioned above pullulan, but well below those of alginate and hyaluronan. The vertical shift (or equivalently the horizontal shift) depends on the chain stiffness, e.g. the persistence length (q), as well as the mass per unit length (M_L). Given the latter, the former can be estimated from R_G-M data by the Benoit-Doty model for wormlike chains (see e.g. ref. (Mendichi, Soltes & Schieroni, 2003) for its application on hyaluronan or ref. (Vold, Kristiansen & Christensen, 2006) for alginates). In the present case the situation is simplified by the absence of polyelectrolyte effects.

To apply the Benoit-Doty model an average value for the mass per unit length (M_L) must be known. It is given by Eq. 1.

$$M_L = \frac{M_0}{l_0} \qquad (1)$$

Here, M_0 is the molar mass of the repeating unit, whereas l_0 is the corresponding contour length. As a first approximation for l_0 the sum of the lengths of the individual sugars in the backbone is estimated by comparison to published values of related polysaccharides. The value for THS is expected to be close to that of HA (Mendichi, Soltes & Schieroni, 2003), i.e. 0.85 nm. For ST1 it should be close to 0.515 nm for the two β-(1→4)-linked residues (taken from cellulose). The β-(1→6)-linked residue could be taken to be 0.515 based on the X-ray diffraction data for the α-(1→4)-linked analogue (dextran) (Stivala & Patel, 1987), whereas the β-(1→3)-linked residue could be taken to be that found in curdlan (Zhang & Nishinari, 2009) (0.23 nm). However, as a second and independent approach the contour lengths of the repeating units were estimated using CarbBuilder (Kuttel, Mao, Widmalm & Lundborg, 2011) as implemented in CASPER(Lundborg, Fontana & Widmalm, 2011). The CarbBuilder estimates tended to be 10-20% above the estimates based on individual residues, suggesting a slight extension of the chains due to side chains. The latter were chosen as basis for determining the persistence lengths (1.0 nm for THS, 1.3 nm for

K16, 1.9 nm for ST1). Based on fitting the R_G-M data to the Benoit-Doty model, the calculated persistence lengths were 9 nm for THS and 10 nm for K16, respectively, whereas for ST1 the results varied from 4.5 nm for the low M end to 5.5 nm for the high M end.

Figure 6 shows plots of the molar mass dependency of the intrinsic viscosity, often termed the Mark-Houwink-Sakurada (MHS) plot. The underlying exponential equation ($[\eta] = KM^a$), where the exponent is zero for polymers shaped as solid spheres, 0.5 for random coils in a θ-solvent, 0.8 for a random coil in a thermodynamically good solvent, and 1.8 for polymers shaped as rigid rods. In the present case fitting of the data provides exponents of 0.65 (THS), 0.62 (K16) and 0.55 (ST1). The values are qualitatively in agreement with those determined from R_G values, i.e. all polysaccharides behave as random coils. It may be noted none of the curves in Figure 6 are perfectly linear, but show a tendency of curvature. This phenomenon is well-known and is mainly attributed to non-Newtonian behaviour (shear thinning) caused by the high shear rates operating in the on-line viscometer (> 1000 s^{-1}), and where the effect increases progressively with increasing molar masses. Hence, fitting the MHS equation using only the lowest molar masses with acceptable intrinsic viscosity data produces slightly higher exponents (0.73, 0.68 and 0.69), yet the values remain within the random coil range. The latter estimate of 0.69 for ST1 is questionable because of a possible influence of aggregates/nanoparticles in the low molar mass tail as discussed above.

Comparison to alginate and pullulan (included in Figure 6) shows that for a given molar mass the three polysaccharides behave much more similar to pullulan than to alginate. Hence, they are not very powerful viscosifiers from a fundamental point of view. To obtain intrinsic viscosities in

the range obtained by e.g. commercial xanthan (6000 ml/g) would require molar masses in the range 10^8 – 10^9 Da.

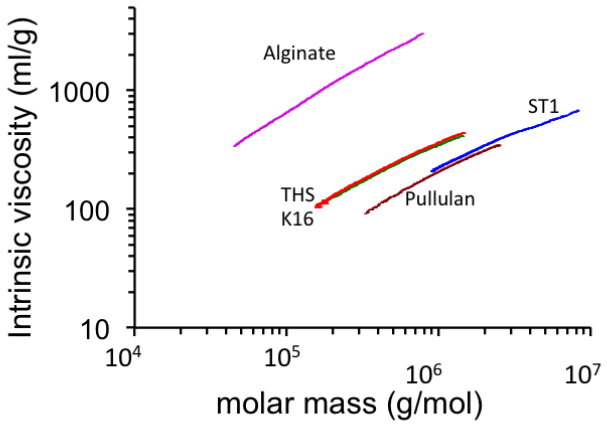

Figure 6. Mark-Houwink-Sakurada plot: Molar mass dependency of the intrinsic viscosity (slice values) for THS (red), K16 (green), ST1 (blue), alginate (magenta), and pullulan (brown). Data at the peak ends providing pronounced deviations or noise were removed prior to analysis.

It is possible to estimate the persistence length also from data such as those given in Figure 6 based on the wormlike chain model. The most common approach is the so-called Bohdanecky approach (Bohdanecky, 1983) affording a simplification (Patel, Picout, Ross-Murphy & Harding, 2006) of the more rigorous analytical expressions in the original theory. According to the theory the parameter $(M^2/[\eta])^{1/3}$ is a linear function of $M^{1/2}$, whereby both M_L and the persistence length can be obtained. Details on the approach as applied to hyaluronan and alginate is given in the literature (Mendichi, Soltes & Schieroni, 2003; Vold, Kristiansen & Christensen, 2006). The 'Bohdanecky plots ' of THS, K16 and ST1 are given in Figure 7. The linear fits were restricted to the lowest molar masses to minimize excluded volume effects, which strictly need to be absent in

order to use the model. The calculated persistence lengths were roughly half of those determined from R_G data, but the order and relative magnitude of the estimates paralleled those obtained from R_G data.

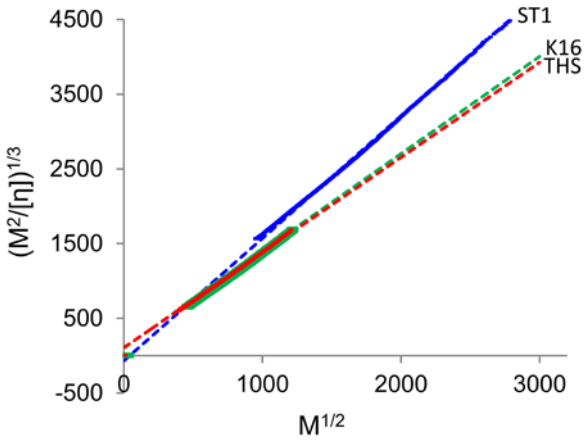

Figure 7. Bohdanecky plots for ST1 (blue), THS (red) and K16 (green).

4 DISCUSSION

The three EPS investigated herein have structural elements in common, viz., first of all the disaccharide β-lactose, secondly the trisaccharide α-D-Glc*p*-(1→4)-β-D-Gal*p*-(1→4)-β-D-Glc*p* making up the backbone of the K16 EPS and branching regions in the THS and ST1 polysaccharides and thirdly the sequence β-D-Gal*p*-(1→4)-β-D-Glc*p*-(1→6)-α-D-Glc*p*-(1→4)-β-D-Gal*p*-(1→4)-β-D-Glc*p*, which is terminated by β-lactose, occurs in both THS and K16, where in the latter structure an additional β-(1→2)-linked glucose residue is present forming a branched side-chain.

These structural elements are also part of other polysaccharides, e.g. in the O-antigens from *Halomonas magadii* strain 21 MI (de Castro, Molinaro, Wallace, Grant & Parrilli, 2003) and

Halomonas stevensii strain S18214 (Pieretti et al., 2011) both of which have a trisaccharide structure of the repeating unit corresponding to the EPS from THS devoid of the terminal lactose entity in the side-chain, i.e., →3)-[α-D-Glc*p*-(1→4)]β-D-Gal*p*-(1→4)-β-D-Glc*p*-(1→, as well as in the CPS from *Klebsiella* type 37 which has a tetrasaccharide RU containing this trisaccharide structural element(Lindberg, Lindqvist, Lönngren & Nimmich, 1977). The EPS from *Lactobacillus delbrueckii* subsp. *bulgaricus* 291 (Faber, Kamerling & Vliegenthart, 2001) has a pentasaccharide RU that corresponds to that of the EPS from K16 devoid of the β-(1→2)-linked glucose residue in the side-chain and this is also the case for the EPS from *Lactobacillus lactis* subsp. *cremoris* B891 (van Casteren, de Waard, Dijkema, Schols & Voragen, 2000) which in addition carries an *O*-acetyl group on the side-chain glucose residue. The backbone structure →4)-α-D-Glc*p*-(1→4)-β-D-Gal*p*-(1→4)-β-D-Glc*p*-(1→ in the K16 EPS is also present as the backbone in the EPS from *Streptococcus macedonicus* Sc 136 having a branched hexasaccharide RU (Vincent, Faber, Neeser, Stingele & Kamerling, 2001), and in the CPS from group B *Streptococcus* types IV, V and VII, all of which have branched hexa- or heptasaccharide RUs (Di Fabio et al., 1989; Kogan, Brisson, Kasper, Vonhunolstein, Orefici & Jennings, 1995; Wessels et al., 1991).

The three polysaccharides THS, K16 and ST1 have molar mass distributions and averages that correspond to many commercial, water-soluble polysaccharides such as alginates and hyaluronan, i.e. in the range 500 – 2000 kDa (M_w). However, they are not particularly powerful viscosifiers. The intrinsic viscosity values in Table 1 are well below those found in commercial viscosifiers, but the polysaccharides have an advantage over polysaccharides such as hyaluronan or alginate in not being salt sensitive due to the non-polyelectrolyte character.

Multi-detector SEC provides both molar masses, radii of gyration and intrinsic viscosities across the chromatographic profiles (elution slices). However, fitting data to exclude the influence of nanoparticles/aggregates introduces some uncertainty, especially in the low M tail and hence, in the M_n estimates. It may be noted that data in Figures 5 and 6 based on non-fitted molar masses, and in cases such as ST1 in particular there may be uncertainty related to the low M tail and therefore the estimates of the scaling exponents and persistence lengths, respectively.

There seems to be little doubt that all three polysaccharides investigated here behave as slightly expanded random coils in solution. Estimates of the chain stiffness in terms of the persistence lengths on the basis of R_G-M data gave values in the range 9-10 nm for THS and K16. This is slightly above that determined for hyaluronan and close to that of alginate, and well above that for pullulan (1.4-3.1 nm) (Adolphi & Kulicke, 1997). Most probably the presence of bulky side chains has a stiffening effect and contributes significantly to the persistence length.

ST1 seems clearly to be more flexible than the other, despite the challenges caused by contaminants present in the low molar mass tail. The main reason for an increasing flexibility is attributed the presence of a flexible (1→6)-linkage in the main chain. The side-chains are also smaller and less bulky in ST1 compared to THS and K16, and may have a relatively smaller stiffening effect.

The literature contains few analyses of size and extension of other polysaccharides from Lactobacilli, and no comparative experimental analyses have to our knowledge been published. Viilian (Yang, Huttunen, Staaf, Widmalm & Tenhu, 1999), the EPS from *Lactococcus lactis* subsp. cremoris SBT 0495 has, however, been subjected to a through physico-chemical study (Higashimura, Mulder-Bosman, Reich, Iwasaki & Robijn, 2000) using several methods. Viilian

has a pentasaccharide repeating unit where the main chain part consists of the trisaccharide →4)-β-D-Glc*p*-(1→4)-β-D-Gal*p*-(1→4)-β-D-Glc*p*-(1→. The middle D-Gal*p* residue is further substituted at O2 by a α-L-Rha*p* side-chain residue, and at O3 by an α-D-Gal*p*-(1→phosphate) side-chain. Due to the phosphodiester entity in the repeating unit of the EPS viilian becomes a polyelectrolyte, in contrast to the three EPS studied here. However, an intrinsic persistence length (corresponding to the absence of repulsive electrostatic forces, which occurs in the limit of infinite ionic strength) of 11.5 nm was obtained for viilian, which is very close to those of THS and K16.

A comparative analysis of two non-ionic EPS from lactobacteria, *Lactobacillus helveticus* Lh59 and *Streptococcus macedonicus* Sc136, based exclusively on molecular modeling, has been published (van Kuik, Vincent, Leeflang, Kroon-Batenburg & Kamerling, 2006). The calculated persistence lengths were 4.5 nm (Lh59) and 8.5 nm (Sc136). The values are within the range observed for the three EPS studied here, the low value obtained Lh59 being attributed to a flexible (1→5)-linkage in the main chain. The modeling also indicated that side-chains, especially the sugar attached directly to the main chain, could both increase or decrease the chain extension, depending on the linkage position and anomeric configuration.

5 CONCLUSIONS

The EPS from three lactic acid bacteria (*S. thermophilus* THS, *L. helveticus* K16 and *S. thermophilus* ST1) behave as randomly coiled polysaccharides in aqueous solutions. The ST1 EPS had the highest M_w (about 2200 kDa) but the lowest persistence length (q = 5 nm) compared to the lower molar mass THS (M_w = 490 kDa, q = 9 nm) and K16 (M_w = 560 kDa, q = 10 nm). The chain stiffness estimates are within the range of many bacterial and plant polysaccharides. The randomly coiled character indicates no defined higher order structures, e.g. multi-stranded structures, under

the conditions used here. Differences in persistence length are well correlated to the presence of particularly flexible linkages in the main chain, in this case the α-(1→6)-linkage present in the ST1 EPS.

Funding Sources

This work was supported by a grant from The Norwegian University of Science and Technology (NT Faculty grant to MØD) and the Swedish Research Council.

References

Adolphi, U., & Kulicke, W. M. (1997). Coil dimensions and conformation of macromolecules in aqueous media from flow field-flow fractionation/multi-angle laser light scattering illustrated by studies on pullulan. *Polymer, 38*(7), 1513-1519.

Bohdanecky, M. (1983). New Method for Estimating the Parameters of the Wormlike Chain Model from the Intrinsic-Viscosity of Stiff-Chain Polymers. *Macromolecules, 16*(9), 1483-1492.

Broadbent, J. R., McMahon, D. J., Welker, D. L., Oberg, C. J., & Moineau, S. (2003). Biochemistry, genetics, and applications of exopolysaccharide production in Streptococcus thermophilus: a review. *J Dairy Sci, 86*(2), 407-423.

Cescutti, P. (2009). Bacterial capsular polysaccharides and exopolysaccharides. In A. P. Moran (Ed.). *Microbial glycobiology: Structures, relevance and applications* (pp. 93-108): Academic Press, Eslevier Inc.

Christensen, B. E., Ulset, A. S., Beer, M. U., Knuckles, B. E., Williams, D. L., Fishman, M. L., Chau, H. K., & Wood, P. J. (2001). Macromolecular characterisation of three barley beta-glucan standards by size-exclusion chromatography combined with light scattering and viscometry: an inter-laboratory study. *Carbohydrate Polymers, 45*(1), 11-22.

Christensen, B. E., Vold, I. M. N., & Vårum, K. M. (2008). Chain stiffness and extension of chitosans and periodate oxidised chitosans studied by size-exclusion chromatography combined with light scattering and viscosity detectors. *Carbohydrate Polymers, 74*, 559–565.

Cleland, R. L., Wang, J. L., & Detweiler, D. M. (1982). Poly-Electrolyte Properties of Sodium Hyaluronate .2. Potentiometric Titration of Hyaluronic-Acid. *Macromolecules, 15*(2), 386-395.

Cowman, M. K., & Matsuoka, S. (2005). Experimental approaches to hyaluronan structure. *Carbohydrate Research, 340*(5), 791-809.

de Castro, C., Molinaro, A., Wallace, A., Grant, W. D., & Parrilli, M. (2003). Structural determination of the O-specific chain of the lipopolysaccharide fraction from the alkaliphilic bacterium Halomonas magadii strain 21 MI. *European Journal of Organic Chemistry*(6), 1029-1034.

De Vuyst, L., & Degeest, B. (1999). Heteropolysaccharides from lactic acid bacteria. *FEMS Microbiol Rev, 23*(2), 153-177.
Di Fabio, J. L., Michon, F., Brisson, J. R., Jennings, H. J., Wessels, M. R., Benedi, V. J., & Kasper, D. L. (1989). Structure of the Capsular Polysaccharide Antigen of Type-Iv Group-B Streptococcus. *Canadian Journal of Chemistry-Revue Canadienne De Chimie, 67*(5), 877-882.
Divya, J. B., Varsha, K. K., Nampoothiri, K. M., Ismail, B., & Pandey, A. (2012). Probiotic fermented foods for health benefits. *Engineering in Life Sciences, 12*(4), 377-390.
Faber, E. J., Kamerling, J. P., & Vliegenthart, J. F. G. (2001). Structure of the extracellular polysaccharide produced by Lactobacillus delbrueckii subsp bulgaricus 291. *Carbohydrate Research, 331*(2), 183-194.
Fontana, C., Li, S. Y., Yang, Z. N., & Widmalm, G. (2015). Structural studies of the exopolysaccharide from Lactobacillus plantarum C88 using NMR spectroscopy and the program CASPER. *Carbohydrate Research, 402*, 87-94.
Higashimura, M., Mulder-Bosman, B. W., Reich, R., Iwasaki, T., & Robijn, G. W. (2000). Solution properties of viilian, the exopolysaccharide from Lactococcus lactis subsp cremoris SBT 0495. *Biopolymers, 54*(2), 143-158.
Ioan, C. E., Aberle, T., & Burchard, W. (2000). Structure properties of dextran. 2. Dilute solution. *Macromolecules, 33*(15), 5730-5739.
Kogan, G., Brisson, J. R., Kasper, D. L., Vonhunolstein, C., Orefici, G., & Jennings, H. J. (1995). Structural Elucidation of the Novel Type-Vii Group-B Streptococcus Capsular Polysaccharide by High-Resolution Nmr-Spectroscopy. *Carbohydrate Research, 277*(1), 1-9.
Kristiansen, K. A., Dalheim, M. Ø., & Christensen, B. E. (2013). Periodate oxidation and macromolecular compaction of hyaluronan. *Pure Appl. Chem, 85*(9), 1893-1900.
Kuttel, M. M., Mao, Y., Widmalm, G., & Lundborg, M. (2011). *Proc. 7th IEEE Int. Conf. eScience*, 395.
Lindberg, B., Lindqvist, B., Lönngren, J., & Nimmich, W. (1977). Structural Studies of Capsular Polysaccharide of Klebsiella Type-37. *Carbohydrate Research, 58*(2), 443-451.
Liu, J. H. Y., Brant, D. A., Kitamura, S., Kajiwara, K., & Mimura, R. (1999). Equilibrium spatial distribution of aqueous pullulan: Small-angle X-ray scattering and realistic computer modeling. *Macromolecules, 32*(25), 8611-8620.
Lundborg, M., Fontana, C., & Widmalm, G. (2011). Automatic Structure Determination of Regular Polysaccharides Based Solely on NMR Spectroscopy. *Biomacromolecules, 12*(11), 3851-3855.
Mendichi, R., Soltes, L., & Schieroni, A. G. (2003). Evaluation of radius of gyration and intrinsic viscosity molar mass dependence and stiffness of hyaluronan. *Biomacromolecules, 4*(6), 1805-1810.
Nordmark, E. L., Yang, Z. N., Huttunen, E., & Widmalm, G. (2005). Structural studies of an exopolysaccharide produced by Streptococcus thermophilus THS. *Biomacromolecules, 6*(1), 105-108.
Nwodo, U. U., Green, E., & Okoh, A. I. (2012). Bacterial Exopolysaccharides: Functionality and Prospects. *International Journal of Molecular Sciences, 13*(11), 14002-14015.
Patel, A., & Prajapati, J. B. (2013). Food and Health Applications of Exopolysaccharides produced by Lactic acid Bacteria. *Adv. Dairy Res., 1*(2), 1-7.
Patel, T. R., Picout, D. R., Ross-Murphy, S. B., & Harding, S. E. (2006). Pressure cell assisted solution characterization of galactomannans. 3. Application of analytical ultracentrifugation techniques. *Biomacromolecules, 7*(12), 3513-3520.

Patrick, O. M. (2012). Lactic acid bacteia in health and disease. *Rwanda Journal of Health Sciences, 1*(1), 39-50.
Pendrill, R., Säwén, E., & Widmalm, G. (2013). Conformation and Dynamics at a Flexible Glycosidic Linkage Revealed by NMR Spectroscopy and Molecular Dynamics Simulations: Analysis of beta-L-Fucp-(1 -> 6)-alpha-D-Glcp-OMe in Water Solution. *Journal of Physical Chemistry B, 117*(47), 14709-14722.
Pieretti, G., Carillo, S., Kim, K. K., Lee, K. C., Lee, J. S., Lanzetta, R., Parrilli, M., & Corsaro, M. M. (2011). O-chain structure from the lipopolysaccharide of the human pathogen Halomonas stevensii strain S18214. *Carbohydrate Research, 346*(2), 362-365.
Popova, M., Molimard, P., Courau, S., Crociani, J., Dufour, C., Le Vacon, F., & Carton, T. (2012). Beneficial effects of probiotics in upper respiratory tract infections and their mechanical actions to antagonize pathogens. *Journal of Applied Microbiology, 113*(6), 1305-1318.
Purwandari, U., Shah, N. P., & Vasiljevic, T. (2007). Effects of exopolysaccharide-producing strains of Streptococcus thermophilus on technological and rheological properties of set-type yoghurt. *International Dairy Journal, 17*(11), 1344-1352.
Quigley, E. M. M. (2010). Prebiotics and probiotics; modifying and mining the microbiota. *Pharmacological Research, 61*(3), 213-218.
Ruas-Madiedo, P. (2014). Biosynthesis and bioactivity of exopolysaccharides produced by probiotic bacteria. *Food oligosaccharides: Production, analysis and bioactivity*, 1-118.
Ruas-Madiedo, P., Medrano, M., Salazar, N., de los Reyes-Gavilan, C. G., Perez, P. F., & Abraham, A. G. (2010). Exopolysaccharides produced by Lactobacillus and Bifidobacterium strains abrogate in vitro the cytotoxic effect of bacterial toxins on eukaryotic cells. *Journal of Applied Microbiology, 109*(6), 2079-2086.
Stivala, S. S., & Patel, A. (1987). Small angle neutron and X-ray sacattering. In S. S. Stivala, Crescenzi, V., Dea, I.C.M. (Ed.). *Industrial polysaccharides. The impact of biotechnology and advanced methodologies.* (pp. 283-304). New Yourk: Gordon and Breach Science Publishers.
Säwén, E., Huttunen, E., Zhang, X., Yang, Z. N., & Widmalm, G. (2010). Structural analysis of the exopolysaccharide produced by Streptococcus thermophilus ST1 solely by NMR spectroscopy. *Journal of Biomolecular NMR, 47*(2), 125-134.
Tanford, C. (1961). *Physical Chemistry of Macromolecules*. New York: John Wiley & Sons.
Ulset, A.-S., Mori, H., Dalheim, M. Ø., Hara, M., & Christensen, B. E. (2014). The influence of amino acids, buffers and pH on the γ-irradiation induced degradation of alginates. *Biomacromolecules, 15*(12), 4590-4597.
van Casteren, W. H. M., de Waard, P., Dijkema, C., Schols, H. A., & Voragen, A. G. J. (2000). Structural characterisation and enzymic modification of the exopolysaccharide produced by Lactococcus lactis subsp cremoris B891. *Carbohydrate Research, 327*(4), 411-422.
van Kuik, J. A., Vincent, S. J. F., Leeflang, B. R., Kroon-Batenburg, L. M. J., & Kamerling, J. P. (2006). Conformational analysis in aqueous solution and estimation of the persistence length of exopolysaccharides produced by Lactobacillus helveticus Lh59 and Streptococcus macedonicus Sc136. *Canadian Journal of Chemistry-Revue Canadienne De Chimie, 84*(4), 730-742.
Vincent, S. J. F., Faber, E. J., Neeser, J. R., Stingele, F., & Kamerling, J. P. (2001). Structure and properties of the exopolysaccharide produced by Streptococcus macedonicus Sc136. *Glycobiology, 11*(2), 131-139.
Vold, I. M. N., Kristiansen, K. A., & Christensen, B. E. (2006). A study of the chain stiffness and extension of alginates, in vitro epimerized alginates, and periodate-oxidized alginates using

size-exclusion chromatography combined with light scattering and viscosity detectors. *Biomacromolecules, 7*, 2136-2146.
Wessels, M. R., Difabio, J. L., Benedi, V. J., Kasper, D. L., Michon, F., Brisson, J. R., Jelinkova, J., & Jennings, H. J. (1991). Structural Determination and Immunochemical Characterization of the Type-V Group-B Streptococcus Capsular Polysaccharide. *Journal of Biological Chemistry, 266*(11), 6714-6719.
Widmalm, G. (2013). A perspective on the primary and three-dimensional structures of carbohydrates. *Carbohydrate Research, 378*, 123-132.
Yang, Z. N., Huttunen, E., Staaf, M., Widmalm, G., & Tenhu, H. (1999). Separation, purification and characterisation of extracellular polysaccharides produced by slime-forming Lactococcus lactis ssp cremoris strains. *International Dairy Journal, 9*(9), 631-638.
Yang, Z. N., Staaf, M., Huttunen, E., & Widmalm, G. (2000). Structure of a viscous exopolysaccharide produced by Lactobacillus helveticus K16. *Carbohydrate Research, 329*(2), 465-469.
Zhang, H. B., & Nishinari, K. (2009). Characterization of the conformation and comparison of shear and extensional properties of curdlan in DMSO. *Food Hydrocolloids, 23*(6), 1570-1578.